Magnetic properties and microstructural observations of oxide coated FeCo nanocrystals before and after compaction

Z. Turgut,[a] N. T. Nuhfer, H. R. Piehler, and M. E. McHenry
Materials Science and Engineering Department, Carnegie Mellon University, Pittsburgh, Pennsylvania 15213

A radio frequency (rf) plasma torch has been used to produce FeCo nanoparticles with a thin protective oxide coating from metal powder precursors. Structural characterization by conventional and synchrotron x-ray diffraction indicated a disordered bcc α-FeCo phase. High resolution transmission electron microscopy revealed spherical particles with several monolayer thick protective oxide coatings. Thermomagnetic measurements were carried out using a superconducting quantum interference device magnetometer and a vibrating sample magnetometer at temperatures between 5 and 1050 K. Antiferromagnetic (exchange bias) coupling was observed due to the presence of the oxide layer. Relatively high coercivities were observed (280 Oe at 5 K and 250 Oe at room temperature). Néel's surface (interface) anisotropy model was employed to explain the origin of the observed coercivities. As produced powders were hot isostatically pressed at 1023 K and 22 ksi for 2 h. Dense structures were observed and compacted particles revealed coercivities as low as 25 Oe at room temperature. © *1999 American Institute of Physics.* [S0021-8979(99)52808-9]

I. INTRODUCTION

Soft magnetic materials for high temperature applications such as in electric aircraft engine components are in demand. Conventional soft magnetic materials cannot meet the demands at elevated temperatures where mechanical creep resistance and magnetic eddy current losses become important material properties. Recent developments in nanocrystalline materials suggest a promising future for these materials at temperatures up to 875 K. A magnetic nanostructure embedded in a highly resistive matrix may offer a solution for core loses. However, superplastic behavior[1] in nanocrystalline materials is still an issue to be solved. As grain size is reduced below a critical size, the deformation mechanism changes from dislocation nucleation and motion to sliding in the grain boundaries. This suggests the idea of developing a composite material where the high resistive intergranular phase would also have enough mechanical strength to meet the desired mechanical properties, be thin enough to ensure neighboring grain coupling, and be stable at elevated temperatures in order to prevent coarsening. This clearly poses a significant materials challenge.

Two routes for synthesizing exchange coupled nanocrystalline materials are crystallization of amorphous precursors and production of free standing nanocrystalline particles through a plasma arc or plasma torch synthesis. In both cases compaction of precursor materials in a dense bulk form is unavoidable.

Here we report on the synthesis of oxide coated FeCo nanoparticles in a rf plasma torch reactor and their ac and dc magnetic properties before and after compaction. The FeCo alloy system was selected because of higher magnetic induction and magnetic transformation temperatures of this system. At first glance, even though freestanding particles exhibit coercivities that are too large for soft applications we have observed reduction in the coercivities after compaction. We explain the origin of the higher coercivities in the oxide-coated particles through the Néel's surface anisotropy model.

II. EXPERIMENT

We have previously described production of graphite-coated FeCo nanoparticles by plasma torch synthesis[2,3] starting with a mixture of Fe–Co metal precursors. For synthesis of the oxide-coated particles, air was introduced into the plasma gas mixture as an oxidation agent. The plasma power was kept at 50 kW and argon flowing at 40 slpm was used as the plasma gas while the sheath gas consisted of 80 slpm of Ar mixed with 9 slpm of hydrogen. The pressure in the reactor was maintained at 250 Torr during the synthesis.

Structural characterization was carried out by conventional and synchrotron x-ray diffraction (XRD) on powder samples. High resolution transmission electron microscopy (HRTEM) was performed on a JEOL JEM4000EX microscope. An AVG HB501 high resolution scanning transmission electron microscope (STEM) equipped with an Oxford energy dispersive x-ray (EDX) for the high resolution elemental mapping and a Philips XI-30FEG field emission scanning electron microscopy (SEM) were employed for morphological observations and statistical characterization of particle sizes. The dc magnetic properties of as-produced powders were studied using a superconducting quantum interference device (SQUID) magnetometer and a vibrating sample magnetometer (VSM) equipped with a furnace that can operate up to temperatures 1300 K.

As produced powders were hot isostatically pressed (HIPed). A powder precursor was first packed into a cylindrical iron container (2 cm diameter and 2.2 cm height with a wall thickness of 0.25 mm) yielding an ~65% packing density under 2.5 ksi pressure. The Fe canisters were sealed by electron beam welding under vacuum and HIPed at 1023 K and 22 ksi pressure for 2 h. A Walker-401 type hysteresisgraph was employed in determining ac magnetic properties on a toroidal sample cut from a compacted material.

[a]Electronic mail: turgut@andrew.cmu.edu

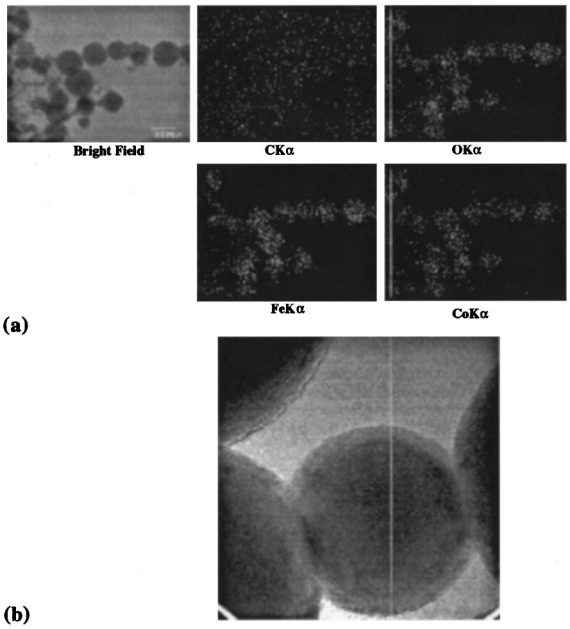

FIG. 1. Elemental mapping (a) and bright field image of as produced particles showing protective ferrite coating around them (b).

III. RESULTS AND DISCUSSION

Initial x-ray diffraction (XRD) structural characterization was carried out using a Rikagu-diffractometer. XRD indicated the presence of bcc FeCo. Further structural analysis by a synchrotron x-ray diffraction revealed that the as formed particles consisted of a disordered bcc α-FeCo phase. The presence of $CoFe_2O_4$ was also detected and was further confirmed in thermomagnetic data. Scherrer analysis of the full width at half maximum (FWHM) indicated an average particle size of 60 nm, that is in good agreement with statistical particle size analysis carried on the SEM images.

Figure 1(a) shows a HRTEM image of as produced particles. Spherical particles with a several atomic layer thick protective $CoFe_2O_4$ were observed. Elemental mapping by EDX indicated homogeneous alloying by plasma torch synthesis and a continuous protective oxide layer formation. A large size distribution was observed ranging from several nanometers to μm size particles. This large size distribution is believed to be due to not having a continuous powder feeding of powder precursors into the plasma stream and having a nonuniform temperature gradient into the reactor vessel. Further effort to keep a continuous powder feed rate yielded particle size distributions between 5 and 200 nm and an average particle size of 27 nm.

Room temperature hysteresis loops taken on the VSM indicated an antiferromagnetic coupling between the host nanoparticles and ferrite coating. Evidence of this came from a shifted (exchange-biased) hysteresis loop. The room temperature specific magnetization was found to be 190 emu/g. Similar to previous reports in oxide-coated nanoparticles[4] relatively high coercivities were observed. SQUID measurements indicated coercivities as high as 280 Oe at 5 K. A strong temperature dependence of the coercivity and saturation magnetization were observed (Fig. 2). The temperature dependence of the coercivity can be explained in part by

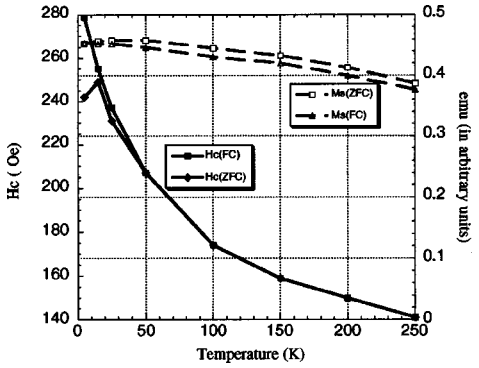

FIG. 2. Temperature dependence of coercivity and saturation magnetization.

considering the temperature dependence of the ferrite coating and host FeCo. As the temperature is increased the magnetic moment in the ferrite is more strongly T-dependent than that of the core FeCo since the Néel temperature of $CoFe_2O_4$ is much lower than the ferromagnetic ordering temperature of FeCo. Due to the diminished exchange coupling between shell and core with increasing temperature, the core becomes magnetically softer resulting in lower coercivities. Differences in field cooled and zero field coercivities support this idea where one can expect higher coercivities in the field cooled state than in the zero field cooled state.

Among various anisotropy terms magnetic surface and interface anisotropy play an important role in determining the magnetic properties of nanocrystalline particles since the surface/volume ratio of these particles are many times larger than that of the bulk materials. This term itself may be able to explain higher coercivities and lower magnetization that are found in many nanocrystalline systems. In this work we have employed Néel's[5] surface and interface anisotropy model in order to explain origin of the observed higher coercivities. In our model we have incorporated the modifications made by O'Handley *et al.*[6]

Néel proposed that atoms in an environment of a reduced symmetry, such as those at a surface or interface, will give rise to anisotropy that is different from the bulk (magnetocrystalline) anisotropy in the material. In this model the elementary or magnetic interaction energy $w(r,\varphi)$ is considered be a function of the separation r (that is the bond distance between two atoms) and the angle between the spontaneous magnetization and the bond axis. This energy is expanded in Legendre polynomials

$$w(r,\varphi)=G(r)+L(r)(\cos^2\varphi-\tfrac{1}{3})+Q(r)(\cos^4\varphi-\tfrac{6}{7}\cos^2\varphi-\tfrac{3}{35})+\ldots.$$

The first term, which is independent of angle φ, includes the spatially isotropic effects such as magnetic exchange $E_{\mathrm{ex}}=-J_{ij}S_I\cdot S_j$. It does not contribute to the magnetic anisotropy. The second, dipolar term describes dipolar anisotropy, and the third quadrupolar anisotropy (the lowest order term present for cubic symmetry). The magnetic anisotropy energy is calculated by summing this interaction energy $w(r,\varphi)$ over all pairs of atoms in the system.

It is obvious that strain is present in these nanoparticles due to the extremely nonequilibrium process conditions and lattice misfit between the host FeCo and the ferrite coating.

In this case the Néel theory needs to be modified to consider magnetoelastic terms. Since it is difficult to accurately determine internal strain in the host, here only strains due to the lattice misfit are considered in the calculations. A MATHEMATICA® code was employed for the calculations. Qualitative anisotropy energy surface plots gives very reasonable results explaining the origin of the canting of the surface moments and higher coercivities found in nanocrystalline powders. For an unstrained bcc bulk material, ⟨100⟩ directions are the easy axes of the magnetization. When magnetization is rotated away from these directions it has higher anisotropy energy. The ⟨110⟩ family has higher anisotropy energy than ⟨100⟩ directions, and ⟨111⟩ is the hard direction for magnetization.

Moments closer to the surface of the particle exhibit different angular dependence to the anisotropy energies than those of the bulk moments far away from the surface. Elongation due to misfit between oxide coating and the host lattice creates an in plane magnetization where [001] becomes the hard direction for magnetization and it can take any direction in the (001) plane. The same kind of effect can also be seen for the atoms that are lying on the (001) plane. Whatever the magnetization direction is, surface moments will prefer to lie in the *x-y* plane. There is no energy difference between the ⟨100⟩ and ⟨110⟩ directions.

For the atomic moments that are on the step-corner sites the ⟨100⟩ directions will be easy. Particularly [100] will be the energetically most favorable direction. Creation of {110} type surfaces is not energetically favorable. While the [110] direction has less anisotropy energy compared to all other directions, it still holds some anisotropy, which makes this type of surface higher energy states. Reduction in coercivity by annealing may be thought of as a result of elimination of internal strains which are due to the synthesis route but the effect of interface anisotropy will always be there.

ac and dc thermomagnetic measurements were also performed on compacted samples up to temperatures of 925 K. A weak temperature dependence was observed and the presence of $CoFe_2O_4$ with a Néel temperature around 520 °C was confirmed as a small bump in $M(T)$. ac magnetic measurements were performed on a toroidal sample with dimensions of 18 mm outer diameter (OD), 16 mm inner diameter (ID), and 2.1 mm thick. Relatively low permeabilities were observed. The temperature dependence of the real and imaginary parts of permeabilities were measured up to 825 K [Figs. 3(a) and 3(b)]. Measurements taken with a 5 Oe field amplitude, and in a 0.1–100 kHz frequency range, revealed that the loss component of the permeability μ'' peaks at 25.1 kHz supporting the idea that presence of high resistance oxide layer keeps eddy current loses low.

Even though a detailed microstructural analysis has not been performed on compacted samples, low values of initial permeabilities are believed to be due to residual porosity rather than a fully dense compact. It should be noted that for ac aircraft applications the permeability requirements are not as high as for other soft magnetic devices. Since the permeability of a magnetic core is reduced as a result of air gap, then the loss factor is reduced proportionally,[7] and one can infer that high loss peak frequencies are not only caused by the oxide shell but also porosity. It was also found that temperature has no effect on peak frequencies for μ'' in these materials. At 600 °C, the peak frequency is found to be the same as that at room temperature. On the other hand, real and imaginary parts of initial permeability were found to be temperature dependent [Fig. 4(b)]. While μ' changes exponentially with temperature, μ'' has a linear dependence. This presumably mimics the temperature dependence of the bulk anisotropy of FeCo.

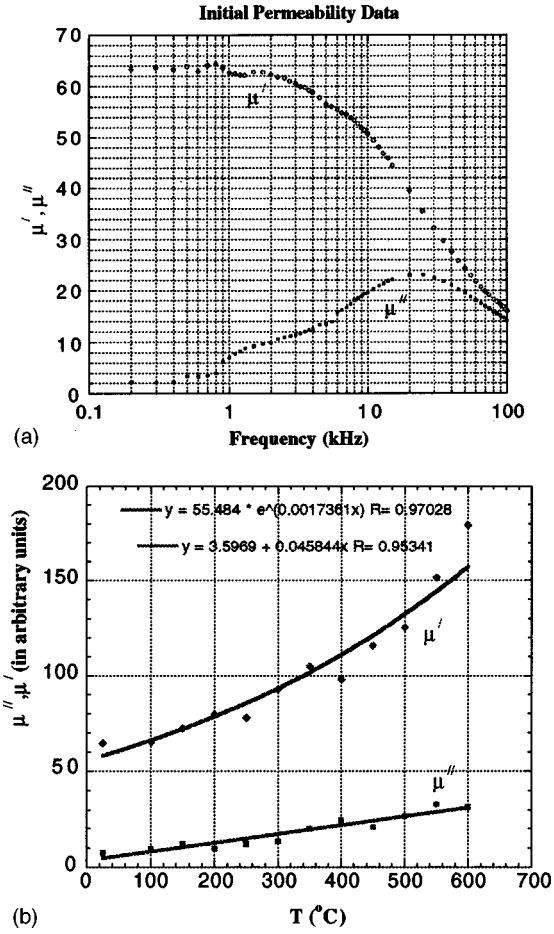

FIG. 3. Real and imaginary parts of initial permeability (a) and temperature dependence of these permeabilities (b).

ACKNOWLEDGMENTS

This work was sponsored by the Air Force Of Scientific Research, Air Force Material Command, USAF, under Grant No. F49620-96-1-0454. The U.S. Government is authorized to reproduce and distribute reprints for governmental purposes notwithstanding any copyright notation thereon.

[1] S. Yip, Nature (London) **391**, 532 (1998).
[2] Z. Turgut, M.-Q. Huang, K. Gallagher, S. A. Majetich, and M. E. McHenry, J. Appl. Phys. **81**, 4039 (1997); Z. Turgut, J. H. Scott, S. A. Majetich, and M. E. McHenry, J. Appl. Phys. **83**, 6468 (1998).
[3] J. H. Scott, Z. Turgut, K. Chowdary, M. E. McHenry, and S. A. Majetich, Mater. Res. Soc. Symp. Proc. **501**, 121 (1998).
[4] S. Gangopadhyay, G. C. Hadjipanayis, C. M. Sorensen, and K. J. Klabunde, Mater. Res. Soc. Symp. Proc. **206**, 55 (1991).
[5] L. Néel, J. Phys. Radium **15**, 225 (1954).
[6] D. S. Chuang, C. A. Ballentine, and R. C. O'Handley, Phys. Rev. B **49**, 15084 (1994).
[7] J. Smith and H. P. J. Wijn, *Ferrites* (Wiley, New York, 1959), p. 123.